Cell and Tissue Research (2019) 378:207–220
https://doi.org/10.1007/s00441-019-03045-3

REGULAR ARTICLE

Synergistic effects of stromal cell-derived factor-1α and bone morphogenetic protein-2 treatment on odontogenic differentiation of human stem cells from apical papilla cultured in the VitroGel 3D system

Min Xiao[1] · Jun Qiu[1] · Rong Kuang[1] · Beidi Zhang[2] · Wei Wang[1] · Qing Yu[1]

Received: 20 October 2018 / Accepted: 27 April 2019 / Published online: 1 June 2019

Abstract

Pulp-dentin regeneration in the apical region of immature permanent teeth represents a significant clinical challenge. Tissue engineering approaches using bioactive molecules and scaffolds may have the potential to regenerate the natural apical structure of these teeth, representing a superior alternative to existing treatment regimens. The aims of this study are (i) to evaluate the VitroGel 3D system, an animal origin-free polysaccharide hydrogel, as a possible injectable scaffold for pulp-dentin regeneration and (ii) to investigate the effects of stromal cell-derived factor-1α (SDF-1α) and bone morphogenetic protein-2(BMP-2) cotreatment on odontogenic differentiation of human stem cells from apical papilla (SCAP) cultured in the VitroGel 3D system. The morphology, viability and proliferation of SCAP cultured in the VitroGel 3D system were measured via scanning electron microscopy (SEM), live and dead cell staining and CCK-8 assays. Alkaline phosphatase (ALP) activity, real-time reverse transcriptase polymerase chain reaction (real-time RT-PCR) and Western blot analysis were further used to evaluate the odontogenic differentiation of SCAP cultured in the VitroGel 3D system in vitro. Finally, the odontogenic differentiation was assessed in vivo through ectopic subcutaneous injection. The results showed that SCAP cultured in 3D hydrogel demonstrated favorable viability and proliferation. SDF-1α and BMP-2 cotreatment enhanced odontogenic differentiation-related gene and protein expression in vitro and promoted odontogenic differentiation of SCAP in vivo. In conclusion, the present study demonstrated that the VitroGel 3D system promoted SCAP proliferation and differentiation. Moreover, SDF-1α cotreatment had synergistic effects on BMP-2-induced odontogenic differentiation of human SCAP cultured in the VitroGel 3D system both in vitro and in vivo.

Keywords Stem cells from apical papilla · Hydrogel · Stromal cell-derived factor-1α · Bone morphogenetic protein-2 · Odontoblastic differentiation

Min Xiao and Jun Qiu contributed equally to this work.

Electronic supplementary material The online version of this article (https://doi.org/10.1007/s00441-019-03045-3) contains supplementary material, which is available to authorized users.

✉ Wei Wang
weiwang3666@hotmail.com

✉ Qing Yu
yuqing@fmmu.edu.cn

[1] State Key Laboratory of Military Stomatology & National Clinical Research Center for Oral Diseases & Shaanxi Key Laboratory of Oral Diseases, Department of Operative Dentistry and Endodontics, The Fourth Military Medical University, Xi'an, China

[2] Department of Endodontics, School of Stomatology, China Medical University, Shenyang, China

Introduction

Pulp necrosis or apical disease arrests further root development of immature permanent teeth, which makes the root canal walls thin and fragile and highly prone to fracture (Lin et al. 2017). Traditional treatment for affected teeth is apexification or apical barriers, which may effectively promote the formation of hard tissue in the apical region but cannot make the root canal longer or the canal wall thicker. The probability of long-term root fracture of these teeth is 28–77% higher than that of normal permanent teeth (Tsesis et al. 2010). Recently, revascularization has attracted significant attention due to its capacity to increase root thickness and, potentially, root length of immature permanent teeth. However, it

has been reported that the tissues generated in the pulp space after revascularization are mainly three types of tissue: intracanal cementum along the dentinal walls, bone-like tissue and periodontal ligament-like tissue (Wang et al. 2010; Chen et al. 2015; Carmen et al. 2017). This type of growth may not result in real pulp-dentin regeneration in the pulp space. Thus, there is significant interest in the exploration of more effective methods to enhance pulp-dentin regeneration in the pulp space of immature permanent teeth. Tissue engineering techniques using bioactive molecules and scaffolds may be able to produce apex regeneration (e.g., pulp-dentin regeneration in the apical region) of immature permanent teeth. SCAP, derived from a developing tissue (apical papilla) in the apical region, have been used as a superior cell source for pulp-dentin regeneration (Lovelace et al. 2011; Huang et al. 2009).

As is well-established, the pulp space (root canal system) is an irregular cavity with a large number of lateral branch root canals and divergent root tips. Within the root canal system, an ideal scaffold should provide adequate root canal modeling and adaptation (Rosa et al. 2013), retain sufficient structural support in the center of the canal space and provide a microenvironmental niche favorable for dental-derived stem cell proliferation and differentiation into odontoblast-like cells (Liu et al. 2018; Chrepa et al. 2017). At present, injectable hydrogel has emerged as a beneficial cell carrier for the repair of irregularly shaped root canal systems and, ultimately, pulp-dentin regeneration (Cavalcanti et al. 2013; Dissanayaka et al. 2015; Muller et al. 2018). In our study, the VitroGel 3D cell culture system, an animal origin-free polysaccharide hydrogel system, was used as a cell carrier for pulp-dentin regeneration. This system closely mimics the natural extracellular matrix (ECM) environment and has been shown to successfully support 3D cultures of various cell types, such as human pancreatic islet cells, human iPSCs and breast cancer cells (Mahauad-Fernandez and Okeoma 2018).

An important morphogenic factor, BMP-2, has not only been shown to promote and maintain osteogenesis (Langer and Vacanti 1993) but is also essential for odontoblast differentiation and dental pulp vascular regeneration (Yang et al. 2017). It has been reported that BMP-2 plays a key role in the differentiation of deciduous tooth stem cells into odontoid cells (Bessa et al. 2008). Furthermore, BMP-2 treatment alone or in combination with collagen matrix on the dental pulp cutting surface can promote the formation of prosthetic dentin (Razzouk and Sarkis 2012; Seo et al. 2015). SDF-1α is a chemokine that belongs to the CXC subfamily, which has been reported to play a critical role in the recruitment, migration and differentiation of hematopoietic stem cells, mesenchymal stem cells (MSC) and endothelial progenitor cells (Zaruba and Franz 2010; Park et al. 2018; De-Colle et al. 2017). Recently, it was reported that SDF-1α promotes odontoblast differentiation of dental pulp cells and the combination of SDF-1α and dental pulp stem cells (DPSC) could promote pulp regeneration in vivo (Nam et al. 2017; Kim et al. 2014). However, the synergistic effects of BMP-2 and SDF-1α on the odontogenic differentiation of human SCAP have not been reported previously. In this study, we investigate the ability of the VitroGel 3D system to serve as an injectable scaffold to promote the proliferation and differentiation of human SCAP. Furthermore, we characterize the effects of cotreatment with BMP-2 and SDF-1α on the odontogenic differentiation of human SCAP cultured in the VitroGel 3D system both in vitro and in vivo.

Materials and methods

Isolation and identification of human SCAP

Disease-free impacted third molars at the stage of root development (from 6 patients aged between 16 and 18 years, male and female) were extracted from patients at the Stomatological Hospital of the Fourth Military Medical University following a protocol approved by the Institutional Review Board of the Fourth Military Medical University. We confirm that all methods were performed in accordance with the relevant guidelines and informed consent was obtained from all patients. Briefly, the extracted teeth were transported in 15 mL centrifuge tubes to the laboratory on ice within 2 h of collection. The apical papilla was isolated from the teeth, minced and digested with 3 mg/mL collagenase type I at 37 °C for 45 min. After washing three times with phosphate-buffered saline (PBS, pH 7.4, Sigma-Aldrich, St Louis, MO, USA), cells were suspended in α-modified of Eagle's Medium (α-MEM, Gibco, Grand Island, NY, USA) supplemented with 10% fetal bovine serum (FBS, Gibco, Australia), 100 U/mL Penicillin and 100 μg/mL streptomycin (Sigma-Aldrich), seeded at a density of 2×10^3 cells/well in 6-well plates and cultured in an incubator at 37 °C in 5% CO_2. The medium was changed every 2 days and cells were passaged when they reached 80% confluence. For immunofluorescence assays, 5×10^3 cells (p4)/coverslip were fixed in 4% paraformaldehyde, permeabilized with 0.5% Triton X-100, blocked with 1% bovine serum albumin (BSA) for 30 min and incubated with primary antibodies against CD105 (1:200 dilution; Santa Cruz Biotechnology, Inc., CA, USA), CD146 (1:200 dilution; Santa Cruz Biotechnology) and STRO-1 (1:200 dilution; R&D Systems Inc., Minneapolis, MN, USA). Dilutions without primary antibodies served as negative control. These incubations were followed by incubation with secondary FITC-conjugated goat-anti-mouse IgG (1:1000 dilution; Abcam, Cambridge, UK) or Cy-3-conjugated goat-anti-mouse IgG (1:2000 dilution; R&D) antibodies; the cell nuclei were stained with 4′,6-diamidino-2-phenylindole (DAPI). All antibodies were used according to the manufacturer's instructions.

Odonto/osteogenic and adipogenic differentiation

Cells were seeded onto 12-well plates at a density of 2×10^4 cells/mL, grown to 70% confluence and incubated in odonto/osteogenic differentiation medium containing 10% FBS, 1% penicillin–streptomycin, 10 nmol/L dexamethasone, 50 mg/L ascorbic acid and 10 nmol/L β-glycerophosphate (all purchased from Sigma-Aldrich) or an adipogenic medium containing 10% FBS, 1% penicillin–streptomycin, 0.1 μM dexamethasone, 0.2 mM indomethacin, 0.01 mg/mL insulin and 0.5 mM IBMX (all purchased from Sigma-Aldrich) for 4 weeks. Cultures were fixed in 4% paraformaldehyde for 30 min, washed and stained with 1% Alizarin Red S (pH = 4.2, Sigma-Aldrich) or 2% Oil red O (Sigma-Aldrich) for 15 min.

Cell viability and proliferation of human SCAP cultured in VitroGel 3D system

VitroGel 3D solution was purchased from TheWell Bioscience (NJ, USA). After preheating to 37 °C, the VitroGel 3D solution was diluted 1:2 with deionized water. Next, the diluted hydrogel solution was gently mixed with cell suspensions using either a microfluid shifter or rapid vortex oscillation. The cell-hydrogel mixture was transferred to 96-well cell culture plates with 50 μL mixture per well and incubated in an atmosphere of 5% CO_2 at 37 °C for 20 min. The final cell concentration of the mixture was 2.5×10^3 cells/well. For 2D cell culture, SCAP were seeded into 96-well plates (2.5×10^3 cells/well) without hydrogel and cultured at 37 °C in an atmosphere of 5% CO_2. Then, 100 μL culture medium was added into every well. The medium was changed every 3 days. At days 0, 1, 4 and 7, 10 μL CCK-8 (Dojindo Laboratories, Kumamoto, Japan) was added into every well and incubated for 3 to 4 h. The absorbance was measured at 450 nm using a microplate reader (Power Wave 340, Bio-TEK, USA).

For live and dead cell staining, the cell-hydrogel mixture was inoculated in an immunofluorescence chamber (5×10^5 cells/well) (Corning Costar, Rochester, NY, USA) and cultured for 4 days. The medium covering the hydrogel was removed. Then, the hydrogel was washed with PBS 3 times. Live and dead cell staining solution (Live-Dead Cell Staining Kit, Biovision, San Francisco, CA, USA) was prepared and added directly to the hydrogel. The solution was incubated at 37 °C for 15 min in the dark. Images were acquired with an Olympus FV1000 confocal microscope (Olympus, Japan) using FV10-ASW3.1 Viewer software via layer-by-layer scanning of the hydrogel mixture. One hundred twenty different layer images were superimposed over one another to create a composite image.

Scanning electron microscopy

Six hundred microliters of mixture was seeded into 24-well plates (2×10^5 cells/well) and cultured for 24 h at 37 °C in an atmosphere of 5% CO_2. Samples were taken at days 1, 4 and 7. The samples were rinsed in deionized water, fixed with 2.5% glutaraldehyde overnight, freeze-dried at − 80 °C overnight and then transferred into a freeze-dryer (FD5–2.5 SIM) for 24 h. The specimens were then sputter-coated with gold and observed under a scanning electron microscope (Hitachi S3400 N, Japan) at an accelerating voltage of 10 kV.

Real-time RT-PCR

A 700 μL mixture was inoculated into 12-well plates (5×10^5 cells/well). The experimental groups were divided into 4 groups: a BMP-2 group, an SDF-1α group, a BMP-2+SDF-1α group and a control group without stimulation. The concentrations of recombinant human BMP-2 protein (PeproTech, Inc., USA) and recombinant human SDF-1α protein (PeproTech) were both 100 ng/mL. The BMP-2+SDF-1α group was treated with SDF-1α for 2 h at 37 °C prior to BMP-2 stimulation. Total RNA from each mixture was extracted using Trizol (Takara Bio Inc., Shiga, Japan) at days 3, 7 and 14 following the manufacturer's protocol and cDNA was synthesized using a Prime Script RT reagent kit (Takara, Dalian, China). The expression levels of target genes were quantified by real-time RT-PCR using a SYBR Premix Ex Taq II kit (Takara) and determined using an ABI 7500 Real-Time PCR System (Biosystems 7500 System, Foster City, CA, USA). The primer sequences of the target genes are listed in Table 1. RNA expression was normalized to GAPDH expression. All reactions were assessed in triplicate.

ALP activity assay

A 500 μL mixture was inoculated into 24-well plates (2×10^5 cells/well). The experimental groups were the same as described previously for real-time RT-PCR assays. At days 3, 7, 11 and 14, the ALP activity of each well was assayed using an ALP kit (Beyotime, Shanghai, China). The mixture was washed twice with PBS and lysed with 50 μL RIPA lysate (Beyotime). After cracking on ice for 5 min, the lysed solution was centrifuged at 12,000*g*/min at 4 °C for 10 min. The supernatant was isolated to determine the total ALP protein level and activity according to the manufacturer's protocol. The optical density (OD) was determined using a microplate reader (Power Wave 340, Bio-TEK, USA) at an absorbance of 405 nm.

Table 1 Real-time RT-PCR primers

Genes	Forward primer	Reverse primer
ALP	CCAAGGACGCTGGGAAATCT	TATGCATGAGCTGGTAGGCG
Runx-2	CCCGTGGCCTTCAAGGT	CGTTACCCGCCATGACAGTA
BSP	GCGAAGCAGAAGTGGATGAAA	TGCCTCTGTGCTGTTGGTACTG
DMP-1	ACTGTGGAGTGACACCAGAA CACA	AGCTGCAAAGTTATCATGCA GATCC
DSPP	GCATTTGGGCAGTAGCATGG	CTGACACATTTGATCTTGCTAGGAG
OCN	GCCAGGCAGGTGCGAAGC	GTCAGCCAACTCGTCACAGTCC
GAPDH	GCACCGTCAAGGCTGAGAAC	TGGTGAAGACGCCAGTGGA

Western blot assay

A 700 μL mixture was inoculated into 12-well plates (2×10^5 cells/well). The experimental groups were the same as described previously for the real-time RT-PCR and alkaline phosphatase activity assays. SCAP were incubated in medium without BMP-2 or SDF-1α as a control group. At days 3 and 14, the samples were lysed in RIPA buffer supplemented with protease inhibitors and subjected to ultrasonication at a low frequency. Supernatants containing total proteins were harvested after centrifugation and the protein concentrations were measured via bicinchoninic acid protein assay (Beyotime). Primary antibodies against runt-related transcription factor 2 (Runx-2) (12556, Cell Signaling Technology, MA, USA), dentin matrix protein 1 (DMP-1) (ab103203, Abcam), dentin sialophosphoprotein (DSPP) (sc-73632, Santa Cruz Biotechnology), bone sialoprotein (BSP) (5468, Cell Signaling Technology), osteocalcin (OCN) (sc-73464, Santa Cruz Biotechnology), or GAPDH (8884, Cell Signaling Technology) were used according to the manufacturer's recommendations. Proteins were extracted, resolved by SDS-PAGE and then transferred to 0.22 μm polyvinylidene difluoride (PVDF) membranes. After blocking in QuickBlock™ Blocking Buffer (Beyotime) for 1 h and probing with the indicated primary antibodies at 4 °C overnight, the membranes were rinsed and incubated with dilutions of appropriate secondary antibodies conjugated with horseradish peroxidase (Cell Signaling Technology) for 1 h at room temperature followed by incubation with an enhanced chemiluminescence kit (Bio-Rad, USA) for a few seconds. Signals were captured using a ChemiDoc MP system (Bio-Rad) and Image Lab software (Bio-Rad). GAPDH was used as an internal control.

In vivo odontogenic differentiation of subcutaneous injections

Six hundred microliters of mixture was inoculated into 12-well plates (5×10^5 cells/well). The experimental groups were the same as described previously for real-time RT-PCR experiments. The cell-hydrogel mixture was cultured with BMP-2 (100 ng/mL) or SDF-1α (100 ng/mL) depending on the experimental protocol in vitro for 7 days prior to injection. With the approval of the Experimental Animal Management Committee, 8 immunodeficient nude mice (6 weeks old, NU/NU, Vital River Laboratory Animal Technology, Beijing, China) were used in these experiments. The operative procedures were as follows: 1% pentobarbital sodium was used to anesthetize nude mice. Then, the mixture was randomly injected into subcutaneous pockets of nude mice on both sides of the body lateral to the dorsal midline. Each mouse had two injection sites. After 8 weeks of implantation, experimental animals were euthanized with carbon dioxide. Specimens were harvested and fixed in 4% paraformaldehyde tissue fixation solution overnight. Some specimens were randomly selected from each group for decalcification in 10% EDTA (pH = 7.4) for 3 weeks. After dehydration and paraffin embedding, 4 μm-thick tissue sections were prepared for histological and immunohistochemical examinations. Hematoxylin and eosin (H&E) staining and Masson's trichrome staining were used for histological examination following the manufacturer's protocol.

Some of the specimens were without demineralization to evaluate the hard tissue formation capability. Briefly, undecalcified sections were stained with Von Kossa staining and Image-Pro Plus 7.0 software (Media Cybernetics, Silver Spring, USA) was used to quantitatively analyze the areas of newly mineralized tissue.

For immunohistochemical staining, the sections were washed in PBS three times (5 min/wash) after antigen repairing, followed by peroxidase, serum, avidin and biotin blocking for 15 min each, respectively. Primary antibodies mouse monoclonal antibody against human DSPP [LFMb-21] (1:50 dilution, sc-73632, Santa Cruz Biotechnology), mouse monoclonal antibody against human osteocalcin [OC4-30] (OCN) (1:100 dilution, ab13418, Abcam), rabbit polyclonal antibody against mouse CD31 (1:100 dilution, ab28364, Abcam), or mouse monoclonal against human nuclear antigen antibody [235-1] (1:100 dilution, ab191181, Abcam) were incubated with the sections at 4 °C overnight. A goat anti-mouse or goat anti-rabbit HRP-AEC cell and tissue staining kit (R&D), including a biotinylated secondary antibody, was subsequently applied to the sections according

to the manufacturer's protocol. Dilutions without primary antibodies served as negative controls. The sections were then counterstained with hematoxylin and mounted. Five randomly selected fields from each tissue section ($n = 3$/group) were imaged with a light microscope (Olympus). The number of CD31-positive blood vessels was determined using Image-Pro Plus 7.0 software (Media Cybernetics).

Statistical analyses

Data reported in this study are expressed as the mean ± standard deviation (SD) of at least three independent experiments. Statistical analysis was performed using SPSS Statistics 20.0 software. The statistical significance of the differences between two groups was analyzed by one-way ANOVA or Student's t test at a significance level of $P < 0.05$.

Results

Isolation and characterization of human SCAP

In this study, human SCAP were successfully isolated from the apical papilla. From morphological observation, the primary cells showed clone-like growth after they were incubated for 3 to 4 days. The cultures were notably heterogeneous and contained cells that ranged from narrow and spindle-shaped to large and polygonal (Fig. 1a). Putative stem cells obtained from cell clones that had been grown for 2 weeks were characterized by multiple lineage differentiation testing and immunofluorescence staining. After 4 weeks of odonto/osteogenic or adipogenic induction, small round Alizarin red-positive mineral nodules (Fig. 1b) or red-positive staining lipid droplets (Fig. 1c) formed in the SCAP cultures, indicating their ability to undergo multiple lineage differentiation. Immunofluorescence staining of SCAP revealed that ex vivo–expanded cells positively expressed the mesenchymal surface markers STRO-1 (Fig. 1d–d"), CD105 (Fig. 1e–e") and CD146 (Fig. 1f–f).

In vitro cell viability and proliferation of human SCAP cultured in the VitroGel 3D system

Scanning electron microscopy (SEM) was used to observe SCAP proliferation over 7 days in the VitroGel 3D system (Fig. 2a–b"'). The control group (hydrogel alone without cells) showed a highly interconnective porosity with circular macropores and a sufficient number of interconnected pores (Fig. 2a, b). At day 1, cells in the hydrogel were evenly dispersed as small balls in interconnected pores with a small amount of extracellular matrix (Fig. 2a', b'). At 4 days, the number of round cells increased along with the amount of extracellular matrix increased (Fig. 2a", b"). At 7 days, a large amount of extracellular matrix was secreted by cells entrapped in interconnected pores (Fig. 2a"', b"'). A marked amount of cellular pseudopodium was observed. Cell proliferation assays (Fig. 2d) revealed that cells proliferated faster at days 1, 4 and 7 than that at day 0 in both 3D hydrogel culture and 2D culture ($P < 0.05$). However, no significant differences in cell proliferation were observed between the 3D culture and 2D culture (data not shown). In the live and dead cell staining assays (Fig. 2c), living cells were stained green and dead cells were stained red. A majority of cells in the hydrogel at 4 days were alive, indicating its favorable biocompatibility.

In vitro odontogenic differentiation of human SCAP cultured in the VitroGel 3D system with BMP-2 and SDF-1α treatment

To determine the effects of BMP-2 or SDF-1α on the odontogenic differentiation of SCAP, the expression levels of genes related to the odontogenic differentiation such as ALP, Runx-2, BSP, DMP-1, DSPP and OCN were assayed by real-time RT-PCR (Fig. 3a–f). The expression levels of ALP, Runx-2, BSP, DMP-1 and OCN genes in the treated groups were almost all significantly upregulated compared to their control groups at days 3, 7 and 14 ($P < 0.05$), whereas the difference in expression levels of the DSPP gene between these groups was only significant at days 7 and 14 ($P < 0.05$). Increased expression of ALP and Runx-2 appeared at day 7, whereas elevated expression of BSP, DMP-1, DSPP and OCN appeared at day 14. The expression levels of ALP, Runx-2, DMP-1, DSPP and OCN at day 7 in the BMP-2+SDF-1α group were significantly higher than those in the BMP-2 or SDF-1α groups ($P < 0.05$). The expression levels of ALP, DMP-1 and OCN at day 14 in the BMP-2+SDF-1α group were significantly higher than those in the BMP-2 or SDF-1α groups ($P < 0.05$), whereas the DSPP expression levels were only significantly upregulated at day 14 in the BMP-2+SDF-1α group relative to the SDF-1α group ($P < 0.05$). Interestingly, BSP expression levels were significantly downregulated at day 14 in the BMP-2+SDF-1α group relative to both the BMP-2 and SDF-1α group ($P < 0.05$).

The ALP activity of SCAP in response to BMP-2 or SDF-1α at days 3, 7, 11 and 14 after 14 days of mineralization induction is shown in Fig. 3(g). The ALP activity of all groups increased until day 14, with the exception of day 3. Compared with the control group, treatment with BMP-2 or SDF-1α markedly increased ALP activity at days 11 and 14 ($P < 0.05$); compared with the other groups, the BMP-2+SDF-1α group showed markedly increased ALP activity at day 14 ($P < 0.05$).

When SCAP in hydrogel were treated for 3 days (Fig. 4a, a'), the protein expression level of Runx-2 in SCAP was significantly upregulated in the treated groups relative to their

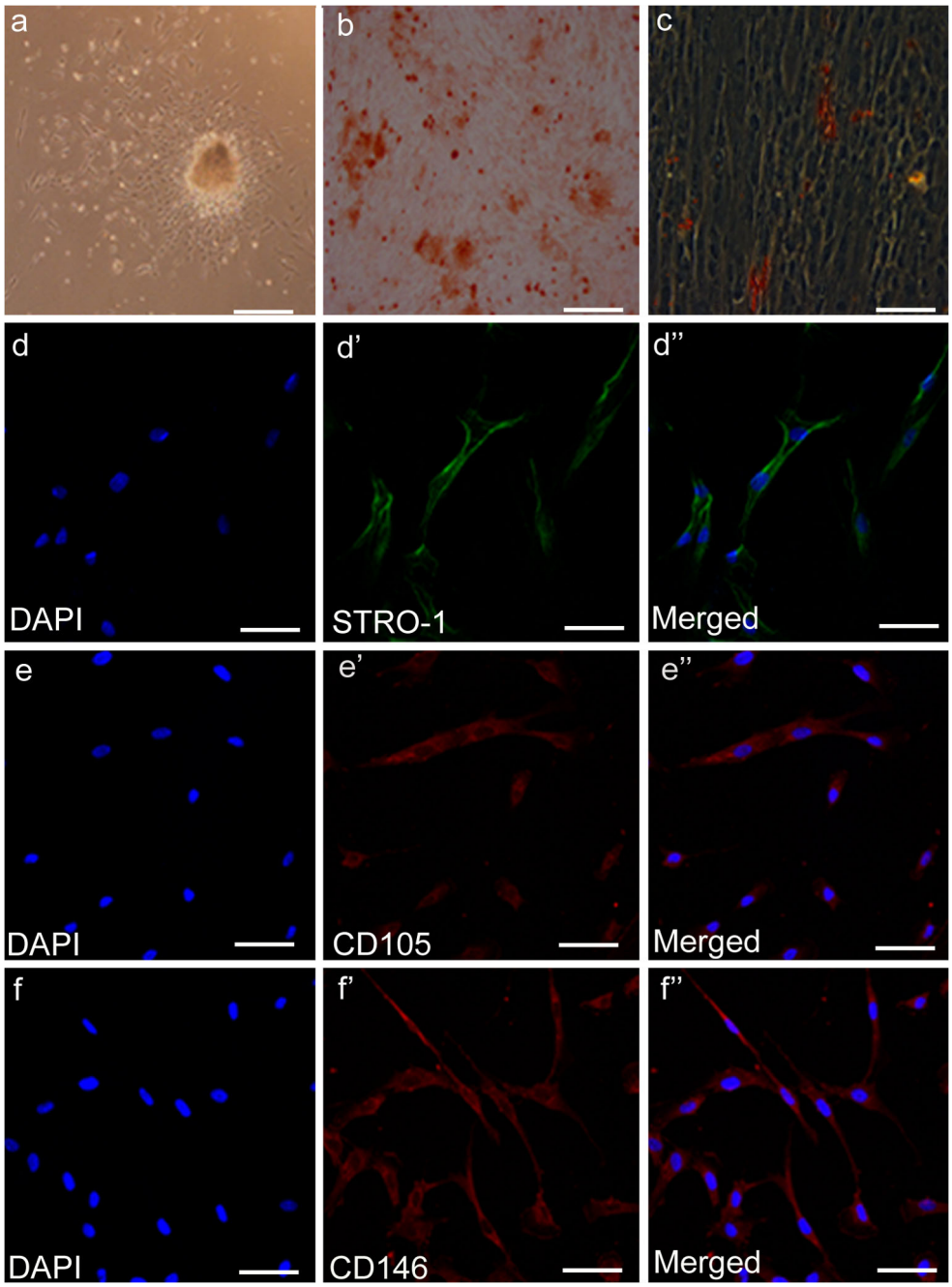

Fig. 1 Multiple lineage differentiation and surface molecule characterization of SCAP. (a) The morphological observation of primary culture SCAP at day 3. (b) Alizarin red S staining for mineralized nodules after odonto/osteogenic induction for 4 weeks. (c) Oil red O staining for lipid droplets after adipogenic induction for 4 weeks. (d–f") Immunofluorescence staining of ex vivo–expanded SCAP revealed positive expression of STRO-1 (d-d"), CD105 (e–e") and CD146 (f–f"). Bars in (a, c), 100 μm; bar in (b), 500 μm; bar in (d–f"), 50 μm

control group ($P < 0.05$). Additionally, the protein expression level of Runx-2 in the BMP-2+SDF-1α group was significantly higher than that in the BMP-2 or SDF-1α group ($P < 0.05$). However, the protein expression level of DMP-1 in the SDF-1α group was significantly elevated compared to either the BMP-2 group or the BMP-2+SDF-1α group at day 3 ($P < 0.05$). After 14 days of treatment (Fig. 4b, b'), the protein expression levels of DMP-1 and DSPP in the BMP-2 group and the BMP-2+SDF-1α group were remarkably upregulated compared to their control group ($P < 0.05$). Moreover, the protein expression levels of DMP-1 and DSPP in the BMP-2+SDF-1α group were significantly higher than those in the SDF-1α group ($P < 0.05$). The protein expression levels of BSP in the BMP-2+SDF-1α group and the SDF-1α group were significantly elevated relative to those in the BMP-2 group at day 3 ($P < 0.05$) (Fig. 4c, c'); however, the levels in the BMP-2+SDF-1α group decreased significantly at day 14 (Fig. 4d, d'). This finding is consistent with the results of the RT-PCR experiments. The protein expression level of OCN was significantly increased in the treated groups relative to the control group at day 3 (Fig. 4c, c'); BMP-2 and SDF-1α treatment significantly enhanced the protein

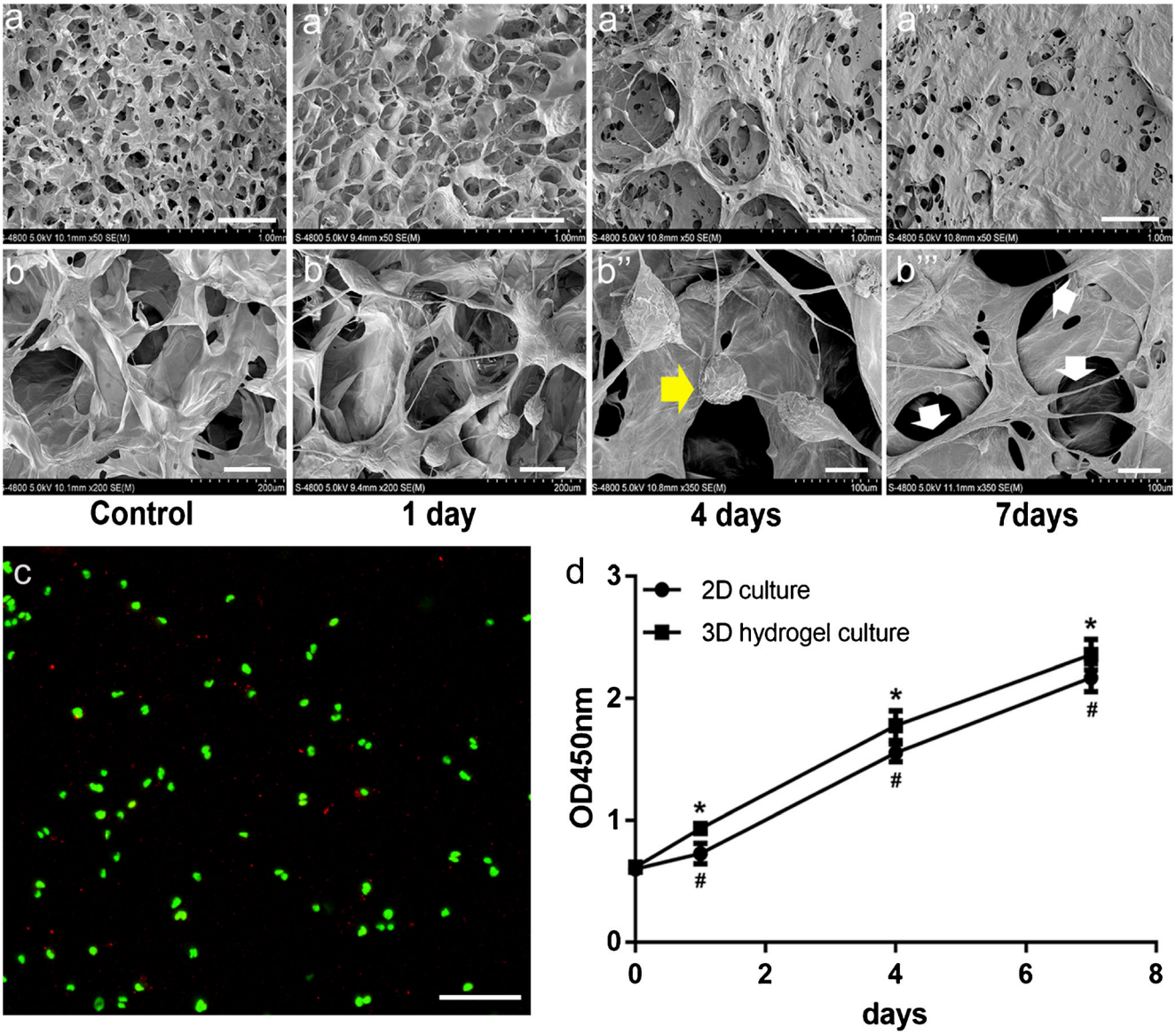

Fig. 2 Proliferation profile of SCAP cultured in the VitroGel 3D system. (a–b''') SEM imaging of SCAP at days 1, 4 and 7 (hydrogel without cells served as the control). The yellow arrow indicates round cells. White arrows indicate cell pseudopodia. Bars in (a–a'''), 500 μm; bar in (b, b'), 100 μm; bar in (b'', b'''), 50 μm; (c) live and dead cell staining of SCAP at day 4. Living cells are stained in green, dead cells are stained in red. Scale bar = 100 μm; (d) quantification of proliferation via CCK-8 assays at days 0, 1, 4 and 7. 3D hydrogel groups compared to their control: $^{*}P < 0.05$. 2D culture groups compared to their control: $^{\#}P < 0.05$

expression level of OCN compared to treatment with either BMP-2 or SDF-1α alone at day 14 ($P < 0.05$) (Fig. 4d, d').

In vivo odontogenic differentiation of human SCAP cultured in the VitroGel 3D system with BMP-2 and SDF-1α pretreatment

Histological examination showed that 8 weeks after injection in nude mice, all specimens were visible to the naked eye and wrapped in a thin membrane. Specimens from the BMP-2 group and the BMP-2+SDF-1α group were encapsulated by thin pink-colored (vascularized) fibrous connective tissues, whereas specimens in the SDF-1α group and control group were encapsulated by thin white-colored fibrous connective tissues. The color of the capsule in the BMP-2+SDF-1α group was richer, with a much more substantial number of vessels on the surface, than that in the BMP-2 group (macroscopic observation, Fig. S1). As shown via H&E staining (Fig. 5a–a'''), osteoid dentin deposits and abundant collagen matrix were found in the BMP-2 group and the BMP-2+SDF-1α group, whereas the mineralization in the SDF-1α group and control group was minimal. The number of osteoid dentin and blood vessels in the BMP-2+SDF-1α group was highest among all of the groups. Masson's trichrome staining (Fig. 5b–b''')

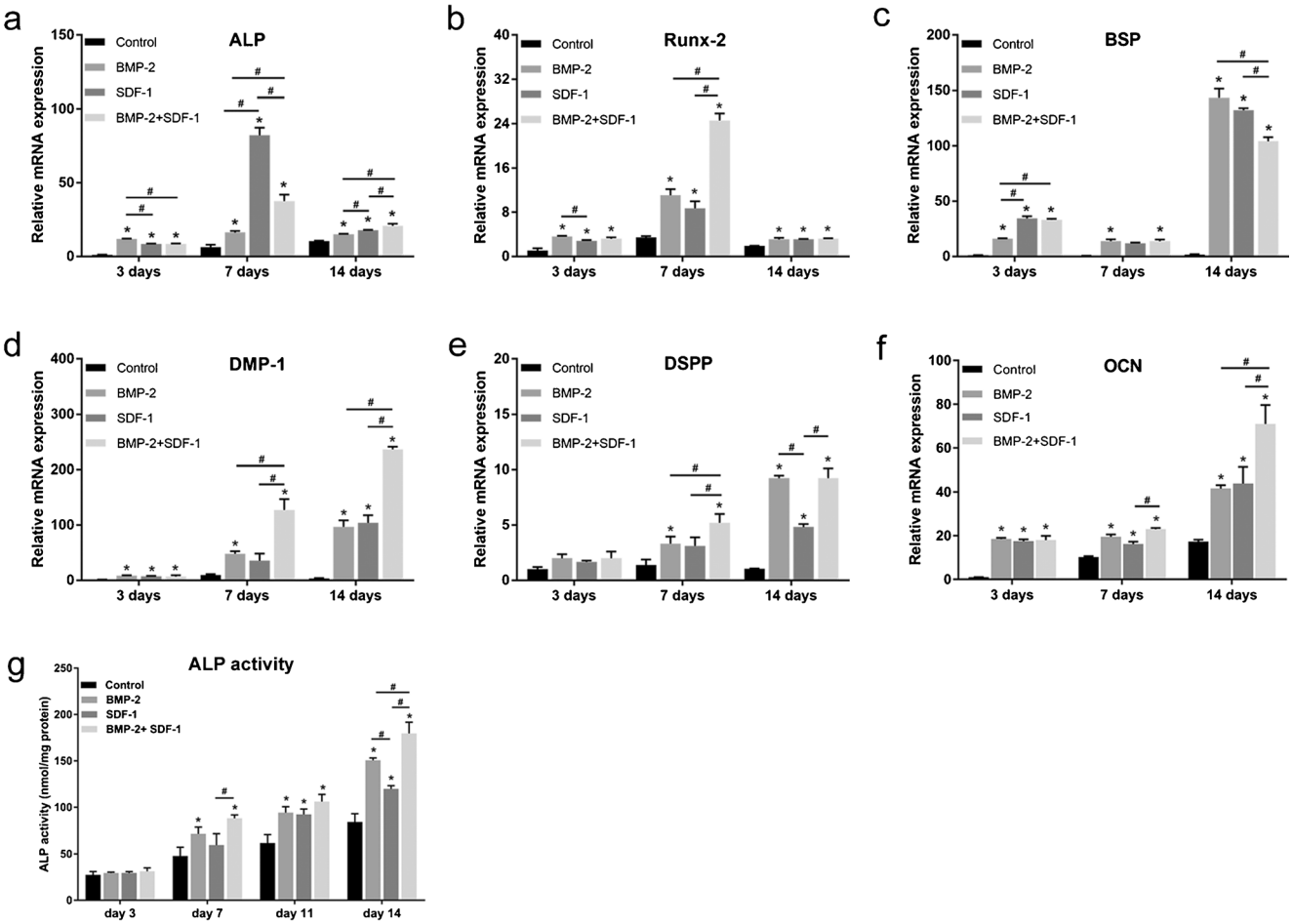

Fig. 3 In vitro odontogenic differentiation of SCAP cultured in VitroGel 3D system with BMP-2 and SDF-1α treatment. Cells were stimulated with 100 ng/mL BMP-2 or pretreated with 100 ng/mL SDF-1α for 2 h at 37 °C before BMP-2 stimulation. Relative gene expression levels of (a–f) ALP, Runx-2, BSP, DMP-1, DSPP and OCN at days 3, 7 and 14. (g) ALP activity quantification at days 3, 7, 11 and 14. The treated groups versus their control group: $^{*}P < 0.05$. Comparison among intragroup: $^{\#}P < 0.05$

showed the newly formed collagen and osteoid dentin, with the collagen stained light blue and the osteoid dentin in dark blue. The level of collagen in the BMP-2+SDF-1α group was higher than in the other groups. Several areas of the BMP-2 group and BMP-2+SDF-1α group were positive for DSPP and OCN protein staining (deep brown areas). In comparison, DSPP protein expression was reduced to barely present in the SDF-1α and control group (Fig. 5c–d"').

To investigate whether BMP-2 and SDF-1α promoted vascularization in vivo, tissue slices from each group were stained with an anti-CD31—a marker for vascular endothelial cells—antibody for immunohistochemical staining (Fig. 6a–a"'). Specimens from all groups except the control group showed positive staining for CD31. A markedly enhanced angiogenic response was evident in the BMP-2+SDF-1α group, resulting in a significantly greater average number of CD31-positive vessels compared to the other groups. Notably, the BMP-2+SDF-1α group had twice the average number of CD31-positive vessels compared with the SDF-1α group (Fig. 6b).

BMP-2 and SDF-1α treatment promote hard tissue regeneration in vivo

Histological examination of the hard tissue constructs 8 weeks after in vivo implantation was performed via Von Kossa staining. High levels of black mineralized tissues were observed in the BMP-2+SDF-1α group and BMP-2 group, which were reduced in the SDF-1α group (Fig. 7a–a"').When analyzed via Image-Pro Plus 7.0 software, the total area of newly mineralized tissues was significantly larger in the BMP-2+SDF-1α group (0.286 ± 0.053 mm^2) compared with the BMP-2 group (0.158 ± 0.028 mm^2) and the SDF-1α group (0.071 ± 0.01 mm^2) ($^{**}P < 0.01$) and the mineralized tissue area identified in the BMP-2 group was significantly more than that in the SDF-1α group ($^{**}P < 0.01$). As expected, no mineralized tissue was observed in the control group (Fig. 7b). As shown in Fig. 7(c,c'), a majority of the nuclei of human cells were stained positively by the antibody for human

nuclear antigen, confirming the human cell origin of the cells in the regenerated hard tissues.

Discussion

Choosing an appropriate scaffold is a critical step for robust tissue engineering strategies, particularly when the scaffold is placed into a small, closed environment, such as the root canal system. To more accurately adhere to physiological pulp cavity morphology, injectable cell carriers have been increasingly used as a new application in dentin tissue engineering scaffolds, including hydrogels, chitosan microspheres and nanofibrous microspheres (Garzon et al. 2018; Huang et al. 2018). However, to date, none of them has been shown to be ideal for the demands of clinical practice. For example, traditional injectable solid microspheres may produce a large number of degradation byproducts and lack biomimetic surface structures to favorably interact with cells (Garzon et al. 2018). Although nanofibrous microspheres could provide advantageous adhesion sites, their biodegradability may not be comparable to injectable hydrogels (Wang et al. 2016). The hydrogel cross-linking network contains a significant amount of water, which can provide sufficient nutrition for cell growth. Moreover, hydrogels not only have superior biocompatibility but can also be injected into the root canal system directly, which reduces operation times and makes for more effective clinical applications. This approach is highly desirable from an endodontic standpoint as injectable scaffolds may conform more easily to the variable shape of a pulp space than a solid or even a moldable scaffold.

In this study, the VitroGel 3D hydrogel system, an animal origin-free polysaccharide hydrogel system, was used as a scaffold for pulp-dentin regeneration. Compared with traditional 2D monolayer cell culture, 3D cell culture technology can more accurately simulate the natural cellular environment in the host organism; these natural conditions can maintain intercellular interactions, as well as more realistic biochemical and physiological reactions. Furthermore, this system is stable at room temperature at a neutral pH and is ready-to-use after simple mixing with cell culture medium, which immediately gelatinizes and stabilizes within 15 min. The speed of the hydrogel formation and its final strength could be altered by different mixing ratios of diluted hydrogel solution and cell culture medium for different clinical applications. SEM imaging showed that the structure and high porosity inside the VitroGel 3D hydrogel system allows for oxygen, nutrition and other molecules to easily enter and leave the hydrogel system. The morphology and behavior of SCAP growth in the 3D hydrogel system is highly similar to the natural growth state (Edmondson et al. 2014). Cells can produce endogenous extracellular matrix proteins and aggregate to form a spherical 3D clone. Moreover, live and dead cell staining experiments demonstrated that SCAP cultured in hydrogel showed favorable viability, with dominant living signals (green) and rarely observed dead signals (red), indicating its high biocompatibility. Moreover, CCK-8 assays showed that SCAP were able to survive and proliferate in the VitroGel 3D hydrogel system under the examined conditions. This sustained cell viability in the hydrogel indicates that an injectable scaffold could conceptually be used in regenerative endodontics (Mahauad-Fernandez and Okeoma 2018; Ferreira et al. 2018).

In addition to suitable scaffold materials, the choice of an appropriate growth factor is also crucial for pulp-dentin regeneration. SDF-1α has been shown to be necessary for tissue repair and regeneration in multiple pathological conditions, such as myocardial infarction (Yu et al. 2010) and acute kidney injury (Togel et al. 2005). With regard to pulp injury and regeneration, SDF-1α reportedly promotes the transmigration and differentiation of dental pulp stem cells (Jiang et al. 2008a, b). As a large number of clinical trials have demonstrated that certain doses of BMP-2 can safely and effectively induce the formation of bone and cartilage in open bone fractures, the application of BMP-2 in dental clinical treatment may be feasible as well (Razzouk and Sarkis 2012). We therefore speculated that compared to treatment with BMP-2 or SDF-1α alone, cotreatment would have more beneficial biological effects on odontogenic regeneration. Our previous study and various other reports had demonstrated that 100 ng/mL BMP-2 remarkably promoted the differentiation of SCAP in monolayer culture but did not significantly affect cell proliferation (Wang et al. 2016). A 100 ng/mL SDF-1α was further shown to promote cell migration without affecting cell proliferation in our pilot study (data not shown). Therefore, we used these concentrations in our further experiments. To investigate the synergistic effects of SDF-1α and BMP-2 on SCAP, the expression levels of various genes related to odontogenic differentiation, ALP activity and protein expression levels were determined. We demonstrated that in vitro SDF-1α treatment enhanced BMP-2-induced ALP activity of SCAP compared with the BMP-2 or SDF-1α groups. ALP is a known marker of early osteoblast and odontoblast differentiation (Harris 1990). Furthermore, Runx-2 has been shown to be an essential factor for early osteogenic/odontogenic differentiation, whereas OCN is a crucial marker of late-stage differentiation (Bruderer et al. 2014). The expression of DSPP can be observed during odontoblastic differentiation (Gu et al. 2013). In addition, DMP-1 is highly expressed in odontoblast, bone and cementum; it may play an important role in the process of dentin mineralization and is considered a specific marker of odontoblast (Gibson et al. 2013). Real-time RT-PCR experiments demonstrated that BMP-2 cotreatment with SDF-1α enhanced the expression of Runx-2, which promoted the early odontogenic differentiation of SCAP and upregulated

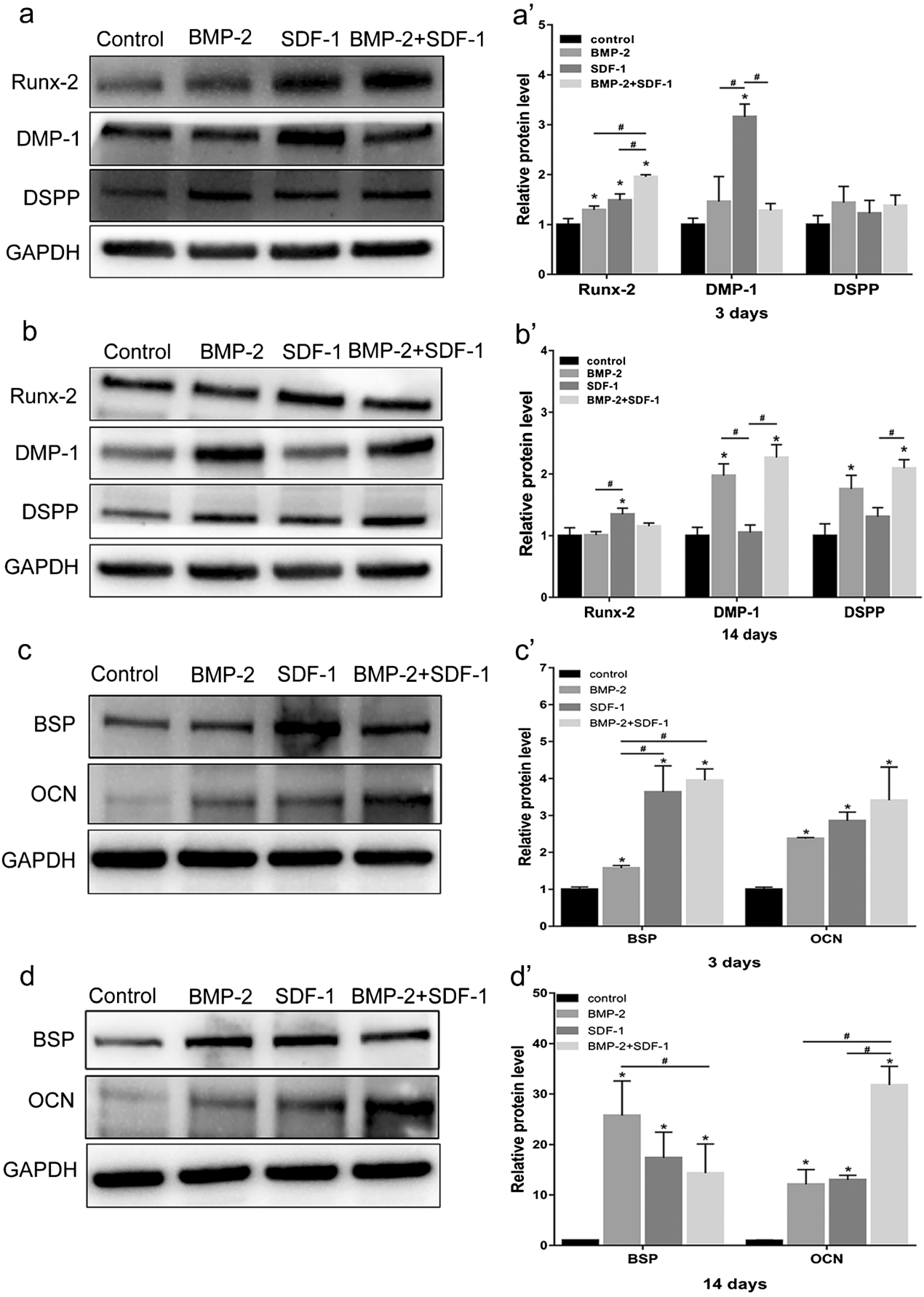
a
Control
BMP-2
SDF-1
BMP-2+SDF-1
Runx-2
DMP-1
DSPP
GAPDH
a'
control
BMP-2
SDF-1
BMP-2+SDF-1
Relative protein level
Runx-2
DMP-1
DSPP
3 days
b
Control
BMP-2
SDF-1
BMP-2+SDF-1
Runx-2
DMP-1
DSPP
GAPDH
b'
control
BMP-2
SDF-1
BMP-2+SDF-1
Relative protein level
Runx-2
DMP-1
DSPP
14 days
c
Control
BMP-2
SDF-1
BMP-2+SDF-1
BSP
OCN
GAPDH
c'
control
BMP-2
SDF-1
BMP-2+SDF-1
Relative protein level
BSP
OCN
3 days
d
Control
BMP-2
SDF-1
BMP-2+SDF-1
BSP
OCN
GAPDH
d'
control
BMP-2
SDF-1
BMP-2+SDF-1
Relative protein level
BSP
OCN
14 days

◀ **Fig. 4** Western blot analysis of the effects of BMP-2 or SDF-1α treatment on the protein expression of Runx-2, DMP-1 and DSPP in SCAP. (a, a') SCAP treated for 3 days. (b, b') SCAP treated for 14 days. (c, c' and d, d') Western blot analysis of the protein expression of BSP and OCN in SCAP for 3 or 14 days, respectively. Data are shown as means ± SD. Treated groups versus their control group: $^{*}P < 0.05$. Comparison between groups: $^{\#}P < 0.05$

the expression of later odontogenic differentiation genes, such as DMP-1, DSPP and OCN. However, in Western blot analysis, SDF-1α did not significantly enhance the protein expression levels of DMP-1 and DSPP in the BMP-2+ SDF-1α group at day 14; the trend of protein expression is consistent with the trend of gene expression. We thought that proteins expression may take longer than genes expression. And this may be due to an insufficient stimulus for protein synthesis. It may be that if we extend the treatment time or increase the treatment concentrations, there may be significant changes (Lee et al. 2015; Zwingenberger et al. 2016). Our results indicated that SDF-1α and BMP-2 have synergistic effects on the odontoblast differentiation of SCAP, which is consistent with previous studies in other cell types (Kim et al. 2014). Zhu et al. demonstrated that SDF-1α is required for osteogenic differentiation induced by BMP-2 in C2C12 and ST2 cells in vitro (Zhu et al. 2007). Hosogane et al. also reported a similar regulatory role of SDF-1α in BMP-2-induced osteogenic differentiation of human and mouse MSCs (Hosogane et al. 2010).

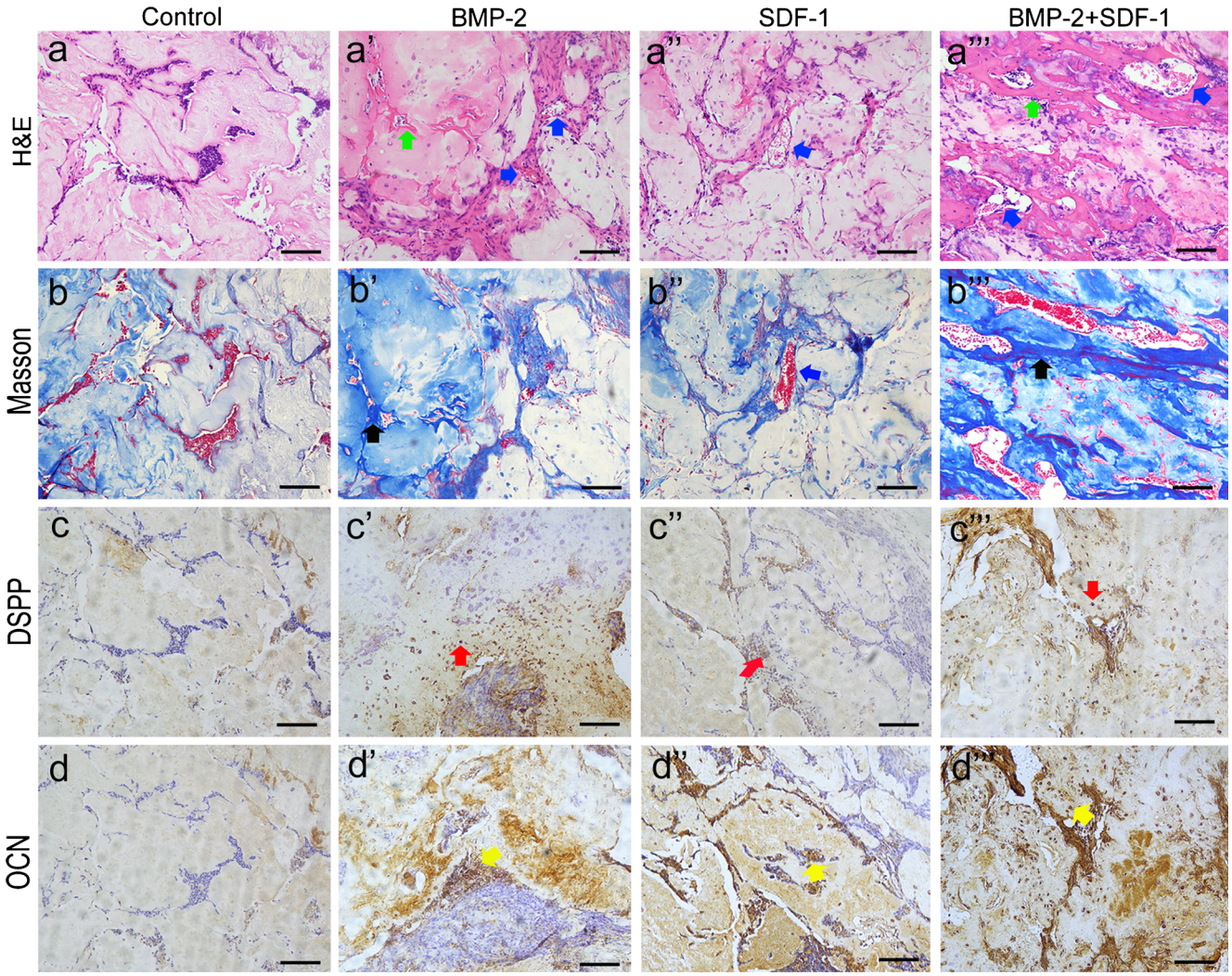

Fig. 5 Histological and immunohistochemical analyses of tissues regenerated in vivo after subcutaneous injection for 8 weeks. (a–a''') H&E staining; (b–b''') Masson's trichrome staining; (c–c''') immunohistochemical staining of DSPP; (d–d''') immunohistochemical staining of OCN. Compared with the control group, the BMP-2 group and the BMP-2 and SDF-1α group formed a marked amount of red collagen matrix (indicated by the green arrow), osteoid dentin (indicated by the black arrow) and vascularization (indicated by the dark blue arrow) in the tissue margin in the H&E staining. The osteoid dentin was stained dark blue and the marked mineralization deposition was observed via Masson's trichrome staining. Positive DSPP protein staining was indicated by the red arrow. Yellow arrows indicate positive OCN protein staining. Scale bar = 100 μm

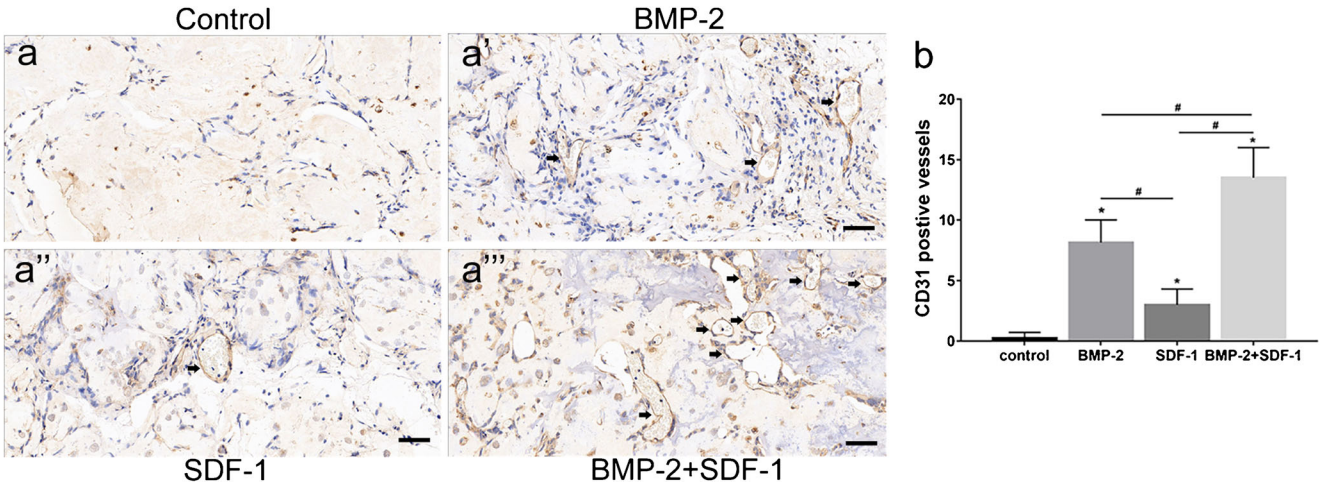

Fig. 6 Immunohistochemical staining for CD31 showed increased vessel formation in the BMP-2+SDF-1α group compared with the other groups. (a–a''') Representative images of CD31-positive vessels (arrows) in the grafts from each group. Scale bar = 50 μm; (b) quantitative analysis of the number of CD31-positive vessels in each group after 8 weeks of implantation. Three samples in each group and five views from each sample were analyzed. The treated groups versus the control group: $^{*}P < 0.05$. Comparisons between groups: $^{\#}P < 0.05$

An appropriate scaffold should be biodegradable and able to facilitate cellular infiltration, vascularization, cell differentiation and eventual replacement by the appropriate tissues. The results of our in vivo experiments revealed that the SDF-1α group did not show significant mineralization, whereas substantial mineralization was observed in the BMP-2+SDF-1α group at week 8. This indicated that SDF-1α might function in differentiation and regeneration in the presence of BMP-2. Furthermore, the presence of red, vascularized, thin fibrous connective tissues in the BMP-2+SDF-1α group indicated abundant angiogenesis, one of the keys to successful tissue engineering. Lataillade et al. showed that SDF-1α treatment could induce proliferation and mediate the mobilization and homing of hematopoietic stem/progenitor cells (Gazitt 2004). Moreover, BMP-2 can stimulate angiogenesis by activating angiogenic signaling pathways. Thus, the additive effects of the cotreatment of SDF-1α and BMP-2 might be explained by potentiated cell mobilization and angiogenesis. In addition, DSPP- and OCN-positive staining were primarily found in the BMP-2 group and BMP-2+SDF-1α group. The combined effects of SDF-1α and BMP-2 improved odontogenic differentiation of

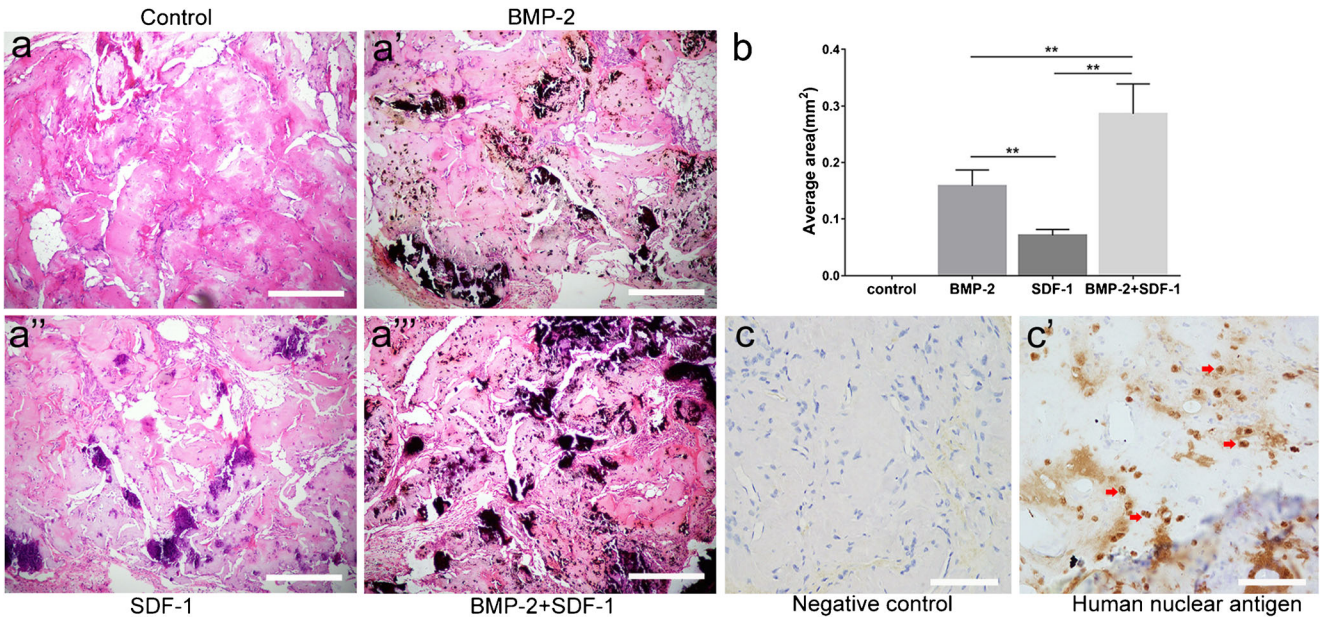

Fig. 7 Histological analysis of hard tissue regeneration in vivo. (a–a''')Von Kossa staining and (b) measurement of the area of newly formed mineralized tissue. (c, c') Immunostaining for human nuclear antigen and negative control with no primary antibody, arrows indicate cells with positive staining. Comparison between groups: $^{**}P < 0.01$, $n = 5$. Bars in (a–a'''), 200 μm; bar in (c, c'), 50 μm

SCAP in vivo, which is consistent with previous reports (Shen et al. 2016; Zwingenberger et al. 2014). Notably, although osteoid-like tissue formations were observed, the formed tissues did not show the typical tubular dentin structure and was quite distinct from actual dentin tissue. This might be attributable to the absence of a suitable microenvironment for odontogenic differentiation. The microenvironment is dynamic and is composed of cells, growth factors and ECM, which directly affects the formation of tissues in vivo. For an odontogenic differentiation environment, the epithelial mesenchymal signals are critically involved in odontogenesis and tubular dentin formation. Microenvironment such as root segment, dentin matrix and various signaling molecules plays an important role in tooth development and formation. Our study only involved subcutaneous implantation in nude mice, which is different from microenvironment in root canal in vivo referring to multiple signal molecules and stem cells. This will be our next study. Further experiments characterizing the VitroGel hydrogel system with growth factors for pulp-dentin engineering are necessary to understand how the hydrogel behaves in regeneration experiments in situ and in relevant clinical conditions. More specifically, it may be important to explore the mechanisms of SDF-1α effects on BMP-2-induced odontogenic differentiation in human SCAP.

In summary, this study provides important evidence that the VitroGel 3D culture system shows good biocompatibility and its injectable characteristics may be applicable in multiple fields. This specific system has many advantages for bridging in vitro and in vivo studies through 3D cell culture and beyond. Our present in vitro and in vivo studies showed that cotreatment of SCAP cultured in the VitroGel 3D system with BMP-2 and SDF-1α had additive effects on odontogenic differentiation. These results indicate that the VitroGel system may serve as a promising scaffold for chair-side regenerative endodontic procedures and may, in concert with other factors, lead to pulp-dentin regeneration.

Acknowledgments We appreciate Beidi Zhang for technical assistance of cell culture and animal experimental and Rong Kuang and Wei Wang for intellectual help on the project.

Funding This study was funded by the National Natural Science Foundation of China (grant numbers 81670975, 31500786, 31600786).

Compliance with ethical standards

Ethical conduct of research All animal procedures were performed and experimental protocols were approved by the guidelines of the Animal Care Committee of the Fourth Military Medical University, Xi'an, China (SCXK (Military) 2007-007), which was in compliance with the NIH Guide for the Care and Use of Laboratory Animals.

Conflict of interest The authors declare that they have no conflict of interest.

References

Bessa PC, Casal M, Reis RL (2008) Bone morphogenetic proteins in tissue engineering: the road from laboratory to clinic, part II (BMP delivery). J Tissue Eng Regen Med 2:81–96

Bruderer M, Richards RG, Alini M, Stoddart MJ (2014) Role and regulation of RUNX2 in osteogenesis. Eur Cells Mater 28:269–286

Carmen L, Asuncion M, Beatriz S, Rosa YV (2017) Revascularization in immature permanent teeth with necrotic pulp and apical pathology: case series. Case Rep Dent 2017:3540159

Cavalcanti BN, Zeitlin BD, Nor JE (2013) A hydrogel scaffold that maintains viability and supports differentiation of dental pulp stem cells. Dent Mater 29:97–102

Chen YP, Jovani-Sancho Mdel M, Sheth CC (2015) Is revascularization of immature permanent teeth an effective and reproducible technique? Dental traumatology : official publication of international association for. Dent Traumatol 31:429–436

Chrepa V, Austah O, Diogenes A (2017) Evaluation of a commercially available hyaluronic acid hydrogel (Restylane) as injectable scaffold for dental pulp regeneration: an in vitro evaluation. J Endod 43:257–262

De-Colle C, Monnich D, Welz S, Boeke S, Sipos B, Fend F, Mauz PS, Tinhofer I, Budach V, Jawad JA, Stuschke M, Balermpas P, Rodel C, Grosu AL, Abdollahi A, Debus J, Bayer C, Belka C, Pigorsch S, Combs SE, Lohaus F, Linge A, Krause M, Baumann M, Zips D, Menegakis A (2017) SDF-1/CXCR4 expression in head and neck cancer and outcome after postoperative radiochemotherapy. Clin Transl Radiat Oncol 5:28–36

Dissanayaka WL, Hargreaves KM, Jin L, Samaranayake LP, Zhang C (2015) The interplay of dental pulp stem cells and endothelial cells in an injectable peptide hydrogel on angiogenesis and pulp regeneration in vivo. Tissue Eng A 21:550–563

Edmondson R, Broglie JJ, Adcock AF, Yang L (2014) Three-dimensional cell culture systems and their applications in drug discovery and cell-based biosensors. Assay Drug Dev Technol 12:207–218

Ferreira SA, Faull PA, Seymour AJ, Yu TTL, Loaiza S, Auner HW, Snijders AP, Gentleman E (2018) Neighboring cells override 3D hydrogel matrix cues to drive human MSC quiescence. Biomaterials 176:13–23

Garzon I, Martin-Piedra MA, Carriel V, Alaminos M, Liu X, D'Souza RN (2018) Bioactive injectable aggregates with nanofibrous microspheres and human dental pulp stem cells: a translational strategy in dental endodontics. J Tissue Eng Regen Med 12:204–216

Gazitt Y (2004) Homing and mobilization of hematopoietic stem cells and hematopoietic cancer cells are mirror image processes, utilizing similar signaling pathways and occurring concurrently: circulating cancer cells constitute an ideal target for concurrent treatment with chemotherapy and antilineage-specific antibodies. Leukemia 18:1–10

Gibson MP, Zhu Q, Wang S, Liu Q, Liu Y, Wang X, Yuan B, Ruest LB, Feng JQ, D'Souza RN, Qin C, Lu Y (2013) The rescue of dentin matrix protein 1 (DMP1)-deficient tooth defects by the transgenic expression of dentin sialophosphoprotein (DSPP) indicates that DSPP is a downstream effector molecule of DMP1 in dentinogenesis. J Biol Chem 288:7204–7214

Gu S, Liang J, Wang J, Liu B (2013) Histone acetylation regulates osteodifferentiation of human dental pulp stem cells via DSPP. Front Biosci (Landmark Ed) 18:1072–1079

Harris H (1990) The human alkaline phosphatases: what we know and what we don't know. Clin Chim Acta 186:133–150

Hosogane N, Huang Z, Rawlins BA, Liu X, Boachie-Adjei O, Boskey AL, Zhu W (2010) Stromal derived factor-1 regulates bone morphogenetic protein 2-induced osteogenic differentiation of primary mesenchymal stem cells. Int J Biochem Cell Biol 42:1132–1141

Huang GT, Gronthos S, Shi S (2009) Mesenchymal stem cells derived from dental tissues vs. those from other sources: their biology and role in regenerative medicine. J Dent Res 88:792–806

Huang L, Xiao L, Jung Poudel A, Li J, Zhou P, Gauthier M, Liu H, Wu Z, Yang G (2018) Porous chitosan microspheres as microcarriers for 3D cell culture. Carbohydr Polym 202:611–620

Jiang HW, Ling JQ, Gong QM (2008a) The expression of stromal cell-derived factor 1 (SDF-1) in inflamed human dental pulp. J Endod 34:1351–1354

Jiang L, Zhu YQ, Du R, Gu YX, Xia L, Qin F, Ritchie HH (2008b) The expression and role of stromal cell-derived factor-1alpha-CXCR4 axis in human dental pulp. J Endod 34:939–944

Kim DS, Kim YS, Bae WJ, Lee HJ, Chang SW, Kim WS, Kim EC (2014) The role of SDF-1 and CXCR4 on odontoblastic differentiation in human dental pulp cells. Int Endod J 47:534–541

Langer R, Vacanti JP (1993) Tissue engineering. Science (New York, NY) 260:920–926

Lee CH, Jin MU, Jung HM, Lee JT, Kwon TG (2015) Effect of dual treatment with SDF-1 and BMP-2 on ectopic and orthotopic bone formation. PLoS One 10:e0120051

Lin J, Zeng Q, Wei X, Zhao W, Cui M, Gu J, Lu J, Yang M, Ling J (2017) Regenerative endodontics versus apexification in immature permanent teeth with apical periodontitis: a prospective randomized controlled study. J Endod 43:1821–1827

Liu W, Lee BS, Mieler WF, Kang-Mieler JJ (2018) Biodegradable microsphere-hydrogel ocular drug delivery system for controlled and extended release of bioactive aflibercept in vitro. Curr Eye Res

Lovelace TW, Henry MA, Hargreaves KM, Diogenes A (2011) Evaluation of the delivery of mesenchymal stem cells into the root canal space of necrotic immature teeth after clinical regenerative endodontic procedure. J Endod 37:133–138

Mahauad-Fernandez WD, Okeoma CM (2018) B49, a BST-2-based peptide, inhibits adhesion and growth of breast cancer cells. Sci Rep 8: 4305

Muller AS, Artner M, Janjic K, Edelmayer M, Kurzmann C, Moritz A, Agis H (2018) Synthetic clay-based hypoxia mimetic hydrogel for pulp regeneration: the impact on cell activity and release kinetics based on dental pulp-derived cells in vitro. J Endod 44:1263–1269

Nam H, Kim GH, Bae YK, Jeong DE, Joo KM, Lee K, Lee SH (2017) Angiogenic capacity of dental pulp stem cell regulated by SDF-1alpha-CXCR4 axis. Stem Cells Int 2017:8085462

Park HJ, Lee WY, Kim JH, Park C, Song H (2018) Expression patterns and role of SDF-1/CXCR4 axis in boar spermatogonial stem cells. Theriogenology 113:221–228

Razzouk S, Sarkis R (2012) BMP-2: biological challenges to its clinical use. N Y State Dent J 78:37–39

Rosa V, Zhang Z, Grande RH, Nor JE (2013) Dental pulp tissue engineering in full-length human root canals. J Dent Res 92:970–975

Seo BB, Choi H, Koh JT, Song SC (2015) Sustained BMP-2 delivery and injectable bone regeneration using thermosensitive polymeric nanoparticle hydrogel bearing dual interactions with BMP-2. J Control Release 209:67–76

Shen X, Zhang Y, Gu Y, Xu Y, Liu Y, Li B, Chen L (2016) Sequential and sustained release of SDF-1 and BMP-2 from silk fibroin-nanohydroxyapatite scaffold for the enhancement of bone regeneration. Biomaterials 106:205–216

Togel F, Isaac J, Hu Z, Weiss K, Westenfelder C (2005) Renal SDF-1 signals mobilization and homing of CXCR4-positive cells to the kidney after ischemic injury. Kidney Int 67:1772–1784

Tsesis I, Rosen E, Tamse A, Taschieri S, Kfir A (2010) Diagnosis of vertical root fractures in endodontically treated teeth based on clinical and radiographic indices: a systematic review. J Endod 36: 1455–1458

Wang X, Thibodeau B, Trope M, Lin LM, Huang GT (2010) Histologic characterization of regenerated tissues in canal space after the revitalization/revascularization procedure of immature dog teeth with apical periodontitis. J Endod 36:56–63

Wang W, Dang M, Zhang Z, Hu J, Eyster TW, Ni L, Ma PX (2016) Dentin regeneration by stem cells of apical papilla on injectable nanofibrous microspheres and stimulated by controlled BMP-2 release. Acta Biomater 36:63–72

Yang G, Yuan G, MacDougall M, Zhi C, Chen S (2017) BMP-2 induced Dspp transcription is mediated by Dlx3/Osx signaling pathway in odontoblasts. Sci Rep 7:10775

Yu J, Li M, Qu Z, Yan D, Li D, Ruan Q (2010) SDF-1/CXCR4-mediated migration of transplanted bone marrow stromal cells toward areas of heart myocardial infarction through activation of PI3K/Akt. J Cardiovasc Pharmacol 55:496–505

Zaruba MM, Franz WM (2010) Role of the SDF-1-CXCR4 axis in stem cell-based therapies for ischemic cardiomyopathy. Expert Opin Biol Ther 10:321–335

Zhu W, Boachie-Adjei O, Rawlins BA, Frenkel B, Boskey AL, Ivashkiv LB, Blobel CP (2007) A novel regulatory role for stromal-derived factor-1 signaling in bone morphogenic protein-2 osteogenic differentiation of mesenchymal C2C12 cells. J Biol Chem 282:18676–18685

Zwingenberger S, Yao Z, Jacobi A, Vater C, Valladares RD, Li C, Nich C, Rao AJ, Christman JE, Antonios JK, Gibon E, Schambach A, Maetzig T, Goodman SB, Stiehler M (2014) Enhancement of BMP-2 induced bone regeneration by SDF-1alpha mediated stem cell recruitment. Tissue Eng A 20:810–818

Zwingenberger S, Langanke R, Vater C, Lee G, Niederlohmann E, Sensenschmidt M, Jacobi A, Bernhardt R, Muders M, Rammelt S, Knaack S, Gelinsky M, Gunther KP, Goodman SB, Stiehler M (2016) The effect of SDF-1alpha on low dose BMP-2 mediated bone regeneration by release from heparinized mineralized collagen type I matrix scaffolds in a murine critical size bone defect model. J Biomed Mater Res A 104:2126–2134